Establishment of a Bernard-Soulier syndrome model in zebrafish

Qing Lin,[1,2*] Riyang Zhou,[1,2*] Panpan Meng,[2*] Liangliang Wu,[2] Lian Yang,[2] Wenyu Liu,[2] Jiaye Wu,[2] Yuhuan Cheng,[1] Linjuan Shi[1] and Yiyue Zhang[1,2]

[1]Key Laboratory of Zebrafish Modeling and Drug Screening for Human Diseases of Guangdong Higher Education Institutes, Department of Developmental Biology, School of Basic Medical Sciences, Southern Medical University and [2]Division of Cell, Developmental and Integrative Biology, School of Medicine, South China University of Technology, Guangzhou, China

**QL, RZ and PM contributed equally as co-first authors.*

Correspondence:

Yiyue Zhang
mczhangyy@scut.edu.cn

Received: March 30, 2021.
Accepted: August 6, 2021.
Prepublished: August 19, 2021.
https://doi.org/10.3324/haematol.2021.278893

Supplementary Materials and Methods

Zebrafish husbandry

Zebrafish adults and embryos were maintained as described previously.[1] The developmental stages were defined according to morphologic criteria.[2] The AB strain, *Tg(cd41:eGFP)*[3] line were utilized. The *gp9* mutants and their WT sibling controls were generated from the progenies of *gp9*^{SMU15} heterozygous parents intercrossing and genotyped after each assay. For *gp9*^{SMU15} mutant with *Tg(cd41:eGFP)* background, *gp9*^{SMU15} homozygous mutants were crossed with *Tg(cd41:eGFP)* homozygous transgenic fish to generate the *Tg(cd41:eGFP);gp9*^{SMU15} double-heterozygotes, which were raised up and collected for parents to produce *Tg(cd41:eGFP);gp9*^{SMU15} mutant and their WT sibling controls for each experiments.

Flow cytometry and cytology analysis

Flow cytometry cell analysis (FACS) were performed as previously described.[4] In detail, whole embryos or larvae were crashed in 0.9 × PBS + 5% FBS solution, and then the tissues were span down and resuspended in 1 mL Dispase (1U/mL) at 37℃ for 20min. Then Hanks buffer (containing 20%FBS, 5mM $CaCl_2$ and DNase) was added to wash the dissociated cells. Similarly, for adult fish, the hematopoietic cells isolated from adult KM and PB were washed and resuspended in 0.9 × PBS plus 5% FBS. Cells were resuspended in 5% FBS and passed through a 40-μm pore-size filter (Falcon) for flow cytometry analysis based on side scatter (SSC) and GFP fluorescence using a flow cytometer (Beckman Coulter Inc, Brea, CA, USA). Meanwhile, *cd41:eGFP*^{high} and *cd41:eGFP*^{low} cells counts and percentages of WT and *gp9*^{SMU15} mutants were

compared by FACS. For each experiment, comparable stages of AB zebrafish were used for non-fluorescence control to set gates. For morphological analyses, the KM cells and sorted *cd41:eGFP*$^{+}$ cells were cytocentrifuged to slides at 400 rpm for 3 minutes and subjected to May-Grünwald and Giemsa (Sigma-Aldrich) staining.

Quantitative real-time polymerase chain reaction (qPCR)

Total RNA was extracted from embryos using TRIzol reagent (Life Technologies, Carlsbad, CA, USA) according to the manufacturer's instructions. The cDNA was generated using MMLV RT for qPCR (Promega, USA). The qPCR was performed with the LightCycler 96 system (Roche, Mountain View, CA, USA) and SYBR Green Master Mix (Applied Biosystems, Carlsbad, CA, USA), according to the manufacturer's instructions. Zebrafish *eef1a1l1 (ef1)* was used as a reference gene. The qPCR primer sets are listed in Supplementary Table. The experiment was duplicated each time and the results were shown as the average of three independent repeats (p values were calculated using the Student *t*-test).

Whole-mount *in situ* hybridization

WISH was performed essentially as described, for *cd41, cmyb, mpo, βe1-globin, rag1, gata1* and *pu.1* probes. Their cRNAs were transcribed *in vitro* by T3 or T7 polymerase (Thermo Fisher Scientific, Waltham, MA, USA) with a digoxigenin-labeled NTP mix (Roche, Basel, Switzerland). Staged embryos were fixed in 4% paraformaldehyde (PFA; Sigma-Aldrich, St Louis, MO, USA) for whole-mount *in situ* hybridization (WISH) with probes according to standard protocols.[5]

O-Dianisidine staining

Embryos were stained for 15 min in the dark with 0.6 mM *O*-Dianisidine staining solution (Sigma-Aldrich), 0.01 M sodium acetate (pH 4.5), 0.65% H_2O_2 and 40% (vol/vol) ethanol as previously described.[6]

Bromodeoxyuridine labeling

Bromodeoxyuridine (BrdU) (Sigma-Aldrich) labeling was performed as described.[7] For GFP and BrdU staining, *Tg(cd41:eGFP)*; wild type (WT) siblings or *Tg(cd41:eGFP)*;*gp9*^{SMU15} embryos were collected at the appropriate stage and fixed in 4% paraformaldehyde. These fixed samples were stained with mouse anti-BrdU (1:50; Roche) and goat anti-GFP (1:200; Abcam, Cambridge, UK), followed by Alexa Fluor donkey anti-mouse-555 (1:400; Invitrogen, Carlsbad, CA, USA) and Fluor donkey anti-goat-488 (1:400; Invitrogen) for fluorescence visualization.

TUNEL assay

TUNEL assay (In Situ Cell Death Detection Kit, TMR Red; Roche) was performed according to the manual, followed by goat anti-GFP (1:200; Abcam) and Alexa Fluor donkey anti-goat-488 (1:400; Invitrogen) for fluorescence visualization.

The *gp9* overexpression

A *hsp-gp9-eGFP* plasmid with a heat-shock promoter was constructed to drive the expression of *gp9* coding DNA sequence (CDS). Zebrafish embryos were injected at one cell stage and heat-shocked at 39°C for 2 hours from 24 to 72 hpf once daily. The larvae with GFP fluorescence were overexpressed successfully, separated and fixed at

3 dpf for WISH.

Statistical analyses

Three test methods were used in this study. Categorical variables were analyzed by Fisher's exact tests. Continuous variables were compared by Student's *t*-test. If the data fitted normal distribution, we chose the Student's *t*-test; if not, we chose a nonparametric test. In all graphs, error bars reflect mean ± SEM. A *P*-value less than 0.05 was considered significant.

Supplementary Figure Legends

Figure S1. Analysis of the thrombocytic cell size in *gp9*^{SMU15} adult zebrafish

(A-C) Flow cytometry analysis and May-Grunwald/Giemsa analysis of KM cells and PB in wild type and *gp9*^{SMU15} fish. FITC was directly proportional to 488-GFP cells and SSC was indicative of cellular granularity. (A) *cd41:eGFP*^{low} and *cd41:eGFP*^{high} thrombocytes in KM cells were sorted and representative cell fluorescence images from each of the cell population gates. (B) *cd41:eGFP*^{high} thrombocytes in PB cells were sorted and representative cell fluorescence images from each of the cell population gates. (C-D) *cd41:eGFP*^{low} and *cd41:eGFP*^{high} thrombocytes in KM (C) and PB (D) cells were sorted and stained by May-Grunwald/Giemsa, representative images from each of the cell population gates. S: small, the cell's diameter is less than 5 μm; M: middle, the cell's diameter is between 5 μm and 10 μm; L: large, the cell's diameter is greater than 10 μm. Quantification of the *cd41:eGFP* positive KM cells (C) and PB cells (D) in wild type and *gp9*^{SMU15} fish. Wild-type *cd41:eGFP*^{low} KM cells: n_L=254, n_M=471; *gp9*^{SMU15} *cd41:eGFP*^{low} KM cells: n_L =110, n_M =206; Wild-type *cd41:eGFP*^{high} KM cells: n_M=42, n_S=49; *gp9*^{SMU15} *cd41:eGFP*^{high} KM cells: n_M=46, n_S=19; Wild-type *cd41:eGFP*^{high} PB cells: n_M=1504, n_S=268; *gp9*^{SMU15} *cd41:eGFP*^{high} PB cells: n_M=620, n_S=30 (Student's *t*-test, n = 3; mean ± SEM; ns, not significant; ** P<0.01, **** P<0.0001).

Figure S2. Myeloid lineage, erythroid and lymphoid are not affected by *gp9* mutation. (A-E) Myeloid, erythroid and lymphoid lineages are not affected in

gp9^{SMU15}mutants. WISH of *mpo* (A), quantification of *mpo*-positive cells in tail (two-sample Student's *t*-test; mean ± SEM; ns: no significance) (B). WISH of *hbbe1* (C, indicated by red arrows) *o*-Dianisidine staining at 5 dpf (D) and WISH of *rag1* (E, indicated by red arrows) expression in 5-dpf WT (left panel) and *gp9*^{SMU15} mutant (right panel).

Figure S3. Primitive blood lineages are not affected by *gp9* mutation. (A-D) Primitive erythroid and myeloid lineages are not affected in *gp9*^{SMU15} mutants. WISH of *hbae1*(A), WISH of *gata1*(B), WISH of *pu.1* (C) and quantification of *pu.1* -positive cells (two-sample Student's *t*-test; mean ± SEM; ns, ns: no significance) (D). The WISH signals were indicated by red arrows in 22-hpf WT (left panel) and *gp9*^{SMU15} mutant (right panel).

Figure S4. Rescue of thrombocytopenia in *gp9*^{SMU15} mutants by *gp9* overexpression. (A) Schematic diagram of the *gp9* overexpression with heat shock treatment. The embryos were injected with *hsp-eGFP* plasmid or *hsp-gp9-eGFP* plasmid at one cell stage and heat-shock once daily after 24 hpi. (B, C) Rescue of *gp9*^{SMU15} mutants. Restoration of *cd41*$^{+}$ cells by heat-shock induced Gp9-eGFP fusion protein overexpression. (B) Representative images of WISH using *cd41* probe in *gp9*^{SMU15} mutants injected with *hsp-eGFP* plasmid for control (upper) or *hsp-gp9-eGFP* plasmid (lower). (C) Quantification (columns) of WISH indicated *cd41*$^{+}$ cells in *gp9*^{SMU15} mutants with *hsp-eGFP* or *hsp-gp9-eGFP*. Statistical significance was determined by two-sample Student's *t*-test, n > 6 mean ± SEM, *** $p < 0.001$ (C).

Figure S5. Phylogenetic tree and proteins alignment analysis of GP9

(A) Evolutionary conservation of GP9. Phylogenetic tree of GP family members among zebrafish, mouse and human based on Maximum Likelihood method and constructed using MEGA program based on the amino acid sequence. Amino acid distance was calculated by using Poisson-corrected mode. The numbers of the branch node represent the bootstrap values. (B) Alignment of GP9 sequence of human, mouse and zebrafish. The GP9 proteins were analyzed with SMART program. LRRNT indicates leucine Rich Repeat N-terminal domain (red box); LRRCT, leucine Rich Repeat C-terminal domain; TM, transmembrane domain (blue box). Alignment of the zebrafish (zGp9), mouse (m*GP9*) and human (hGP9) GP9 amino acid sequences were performed by MEGA program. Sequence marked in underline indicates the ectodomain of human GP9 protein. The black shaded regions of sequence indicate identical residues. The red arrowheads indicate the mutation sites of human *GP9* variant, *hsGP9*$^{70T>C}$ (C24R) and *hsGP9*$^{182A>G}$(N61S).

Supplementary Table

ID Primer	Sequence 5’-3’
gp9 ID primer FP	CAGGATGCTCTTTACTCTTCTCCT
gp9 ID primer RP	CTCAGGCCCTGCAAGC
qRCR Primer	Sequence 5’-3’
cd41 qRCR primer FP	GCTCCTAATGGCTCACAAGTCG
cd41 qRCR primer RP	GCCTCTGGTGTAAATGGCGTCTA
nfe2 qRCR primer FP	GATGCCCATCCTTCTGGTGTATAT
nfe2 qRCR primer RP	CGTGTAGTCATGTTCATGTGCTCC
fog1 qRCR primer FP	CTCCACAGGACAAGCCGAAA
fog1 qRCR primer RP	ACAGGCAAATCAAACAAACAAATG
eef1a1l1 qRCR primer FP	TACTTCTCAGGCTGACTGTG
eef1a1l1 qRCR primer RP	ATCTTCTTGATGTATGCGCT
gp9 qPCR primer FP1	TGACTCCTGCAGGTGCG
gp9 qPCR primer FP2	CATGTCGGCTGTGACTTTGCC
gp9 qPCR primer FP3	AACCTGCTGACCACCATTACTCC
gp9 qPCR primer RP1	TTGGCATCACAGACACTGCTTTAT

Reference:

1. Westerfield M. The Zebrafish Book. A Guide for The Laboratory Use of Zebrafish (Danio rerio), 2000.
2. Kimmel CB, Ballard WW, Kimmel SR, Ullmann B, Schilling TF. Stages of embryonic development of the zebrafish. Dev Dyn. 1995;203(3):253-310.
3. Lin H-F, Traver D, Zhu H, et al. Analysis of thrombocyte development in CD41-GFP transgenic zebrafish. Blood. 2005;106(12):3803-3810.
4. Manoli M, Driever W. Fluorescence-activated cell sorting (FACS) of fluorescently tagged cells from zebrafish larvae for RNA isolation. Cold Spring Harb Protoc. 2012;2012(8):
5. Thisse C, Thisse B. High-resolution in situ hybridization to whole-mount zebrafish embryos. Nat Protoc. 2008;3(1):59-69.
6. Detrich HR, Kieran MW, Chan FY, et al. Intraembryonic hematopoietic cell migration during vertebrate development. Proc Natl Acad Sci U S A. 1995;92(23):10713-10717.
7. Jin H, Li L, Xu J, et al. Runx1 regulates embryonic myeloid fate choice in zebrafish through a negative feedback loop inhibiting Pu.1 expression. Blood. 2012;119(22):5239-5249.

Figure S1

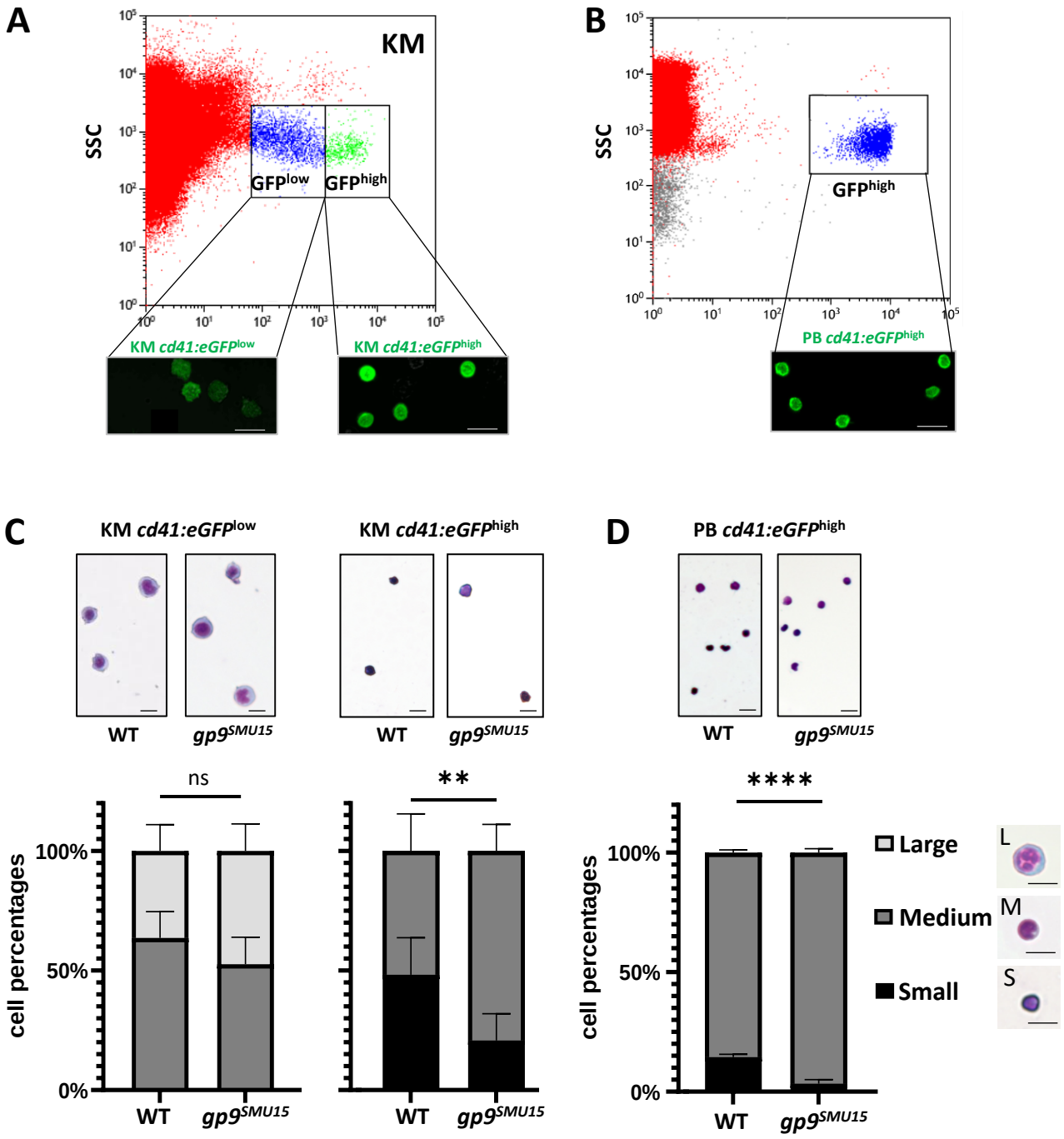
A
KM
SSC
GFPlow
GFPhigh
KM cd41:eGFPlow
KM cd41:eGFPhigh
B
SSC
GFPhigh
PB cd41:eGFPhigh
C
KM cd41:eGFPlow
KM cd41:eGFPhigh
WT
gp9SMU15
ns
**
cell percentages
100%
50%
0%
D
PB cd41:eGFPhigh
****
Large
Medium
Small
L
M
S

Figure S2

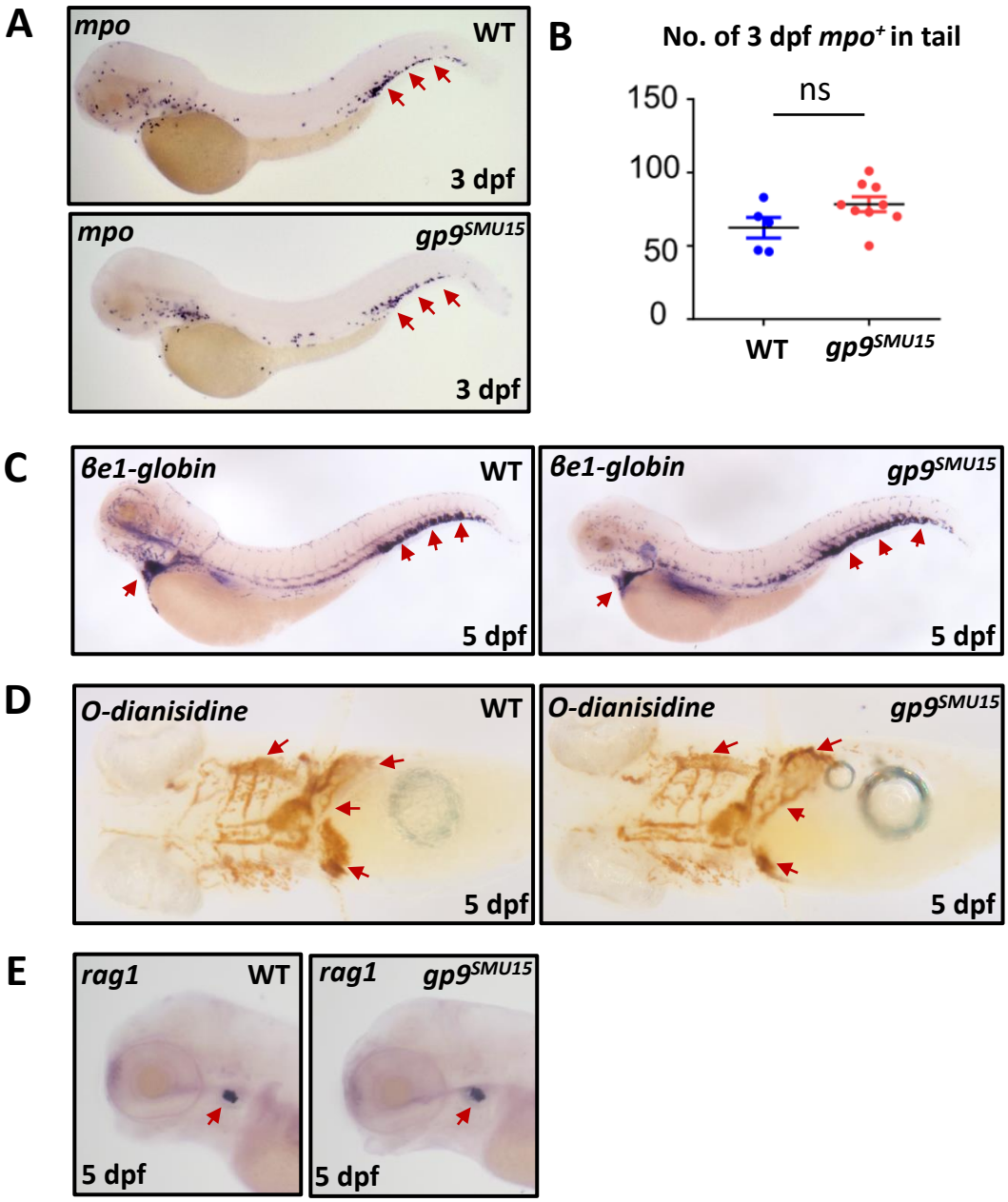
A
mpo
WT
3 dpf
mpo
gp9SMU15
3 dpf
B
No. of 3 dpf mpo+ in tail
ns
150
100
50
0
WT
gp9SMU15
C
βe1-globin
WT
5 dpf
βe1-globin
gp9SMU15
5 dpf
D
O-dianisidine
WT
5 dpf
O-dianisidine
gp9SMU15
5 dpf
E
rag1
WT
5 dpf
rag1
gp9SMU15
5 dpf

Figure S3

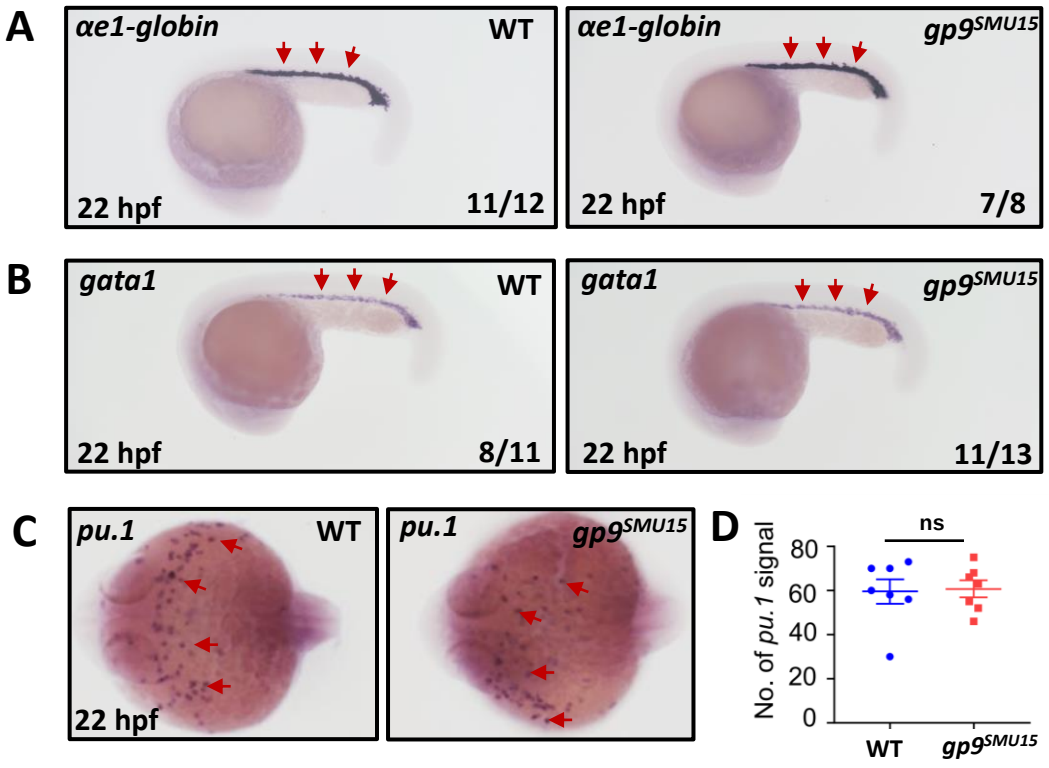
A
αe1-globin
WT
22 hpf
11/12
αe1-globin
gp9SMU15
22 hpf
7/8
B
gata1
WT
22 hpf
8/11
gata1
gp9SMU15
22 hpf
11/13
C
pu.1
WT
22 hpf
pu.1
gp9SMU15
D
ns
No. of pu.1 signal
80
60
40
20
0
WT
gp9SMU15

Figure S4

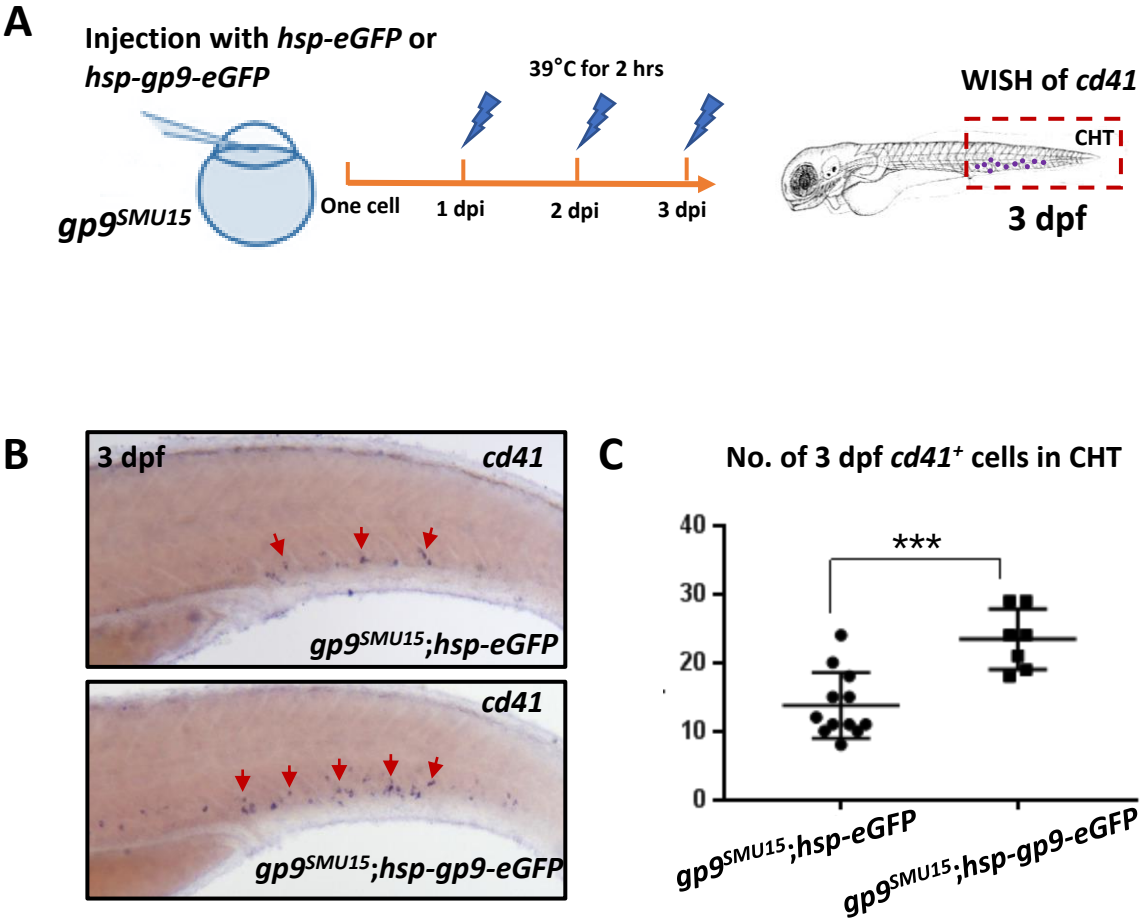
A
Injection with hsp-eGFP or hsp-gp9-eGFP
gp9SMU15
One cell
39°C for 2 hrs
1 dpi
2 dpi
3 dpi
WISH of cd41
CHT
3 dpf
B
3 dpf
cd41
gp9SMU15;hsp-eGFP
cd41
gp9SMU15;hsp-gp9-eGFP
C
No. of 3 dpf cd41+ cells in CHT
***
40
30
20
10
0
gp9SMU15;hsp-eGFP
gp9SMU15;hsp-gp9-eGFP

Figure S5

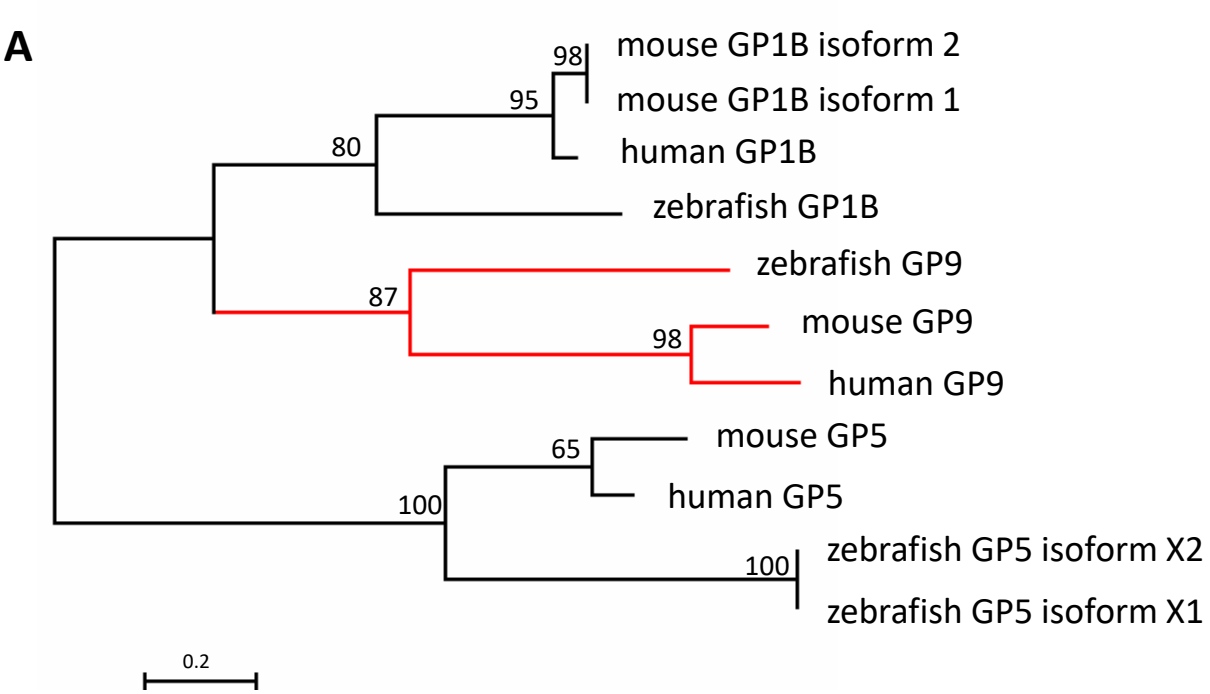
A
98
mouse GP1B isoform 2
95
mouse GP1B isoform 1
80
human GP1B
zebrafish GP1B
zebrafish GP9
87
mouse GP9
98
human GP9
mouse GP5
65
human GP5
100
zebrafish GP5 isoform X2
100
zebrafish GP5 isoform X1
0.2

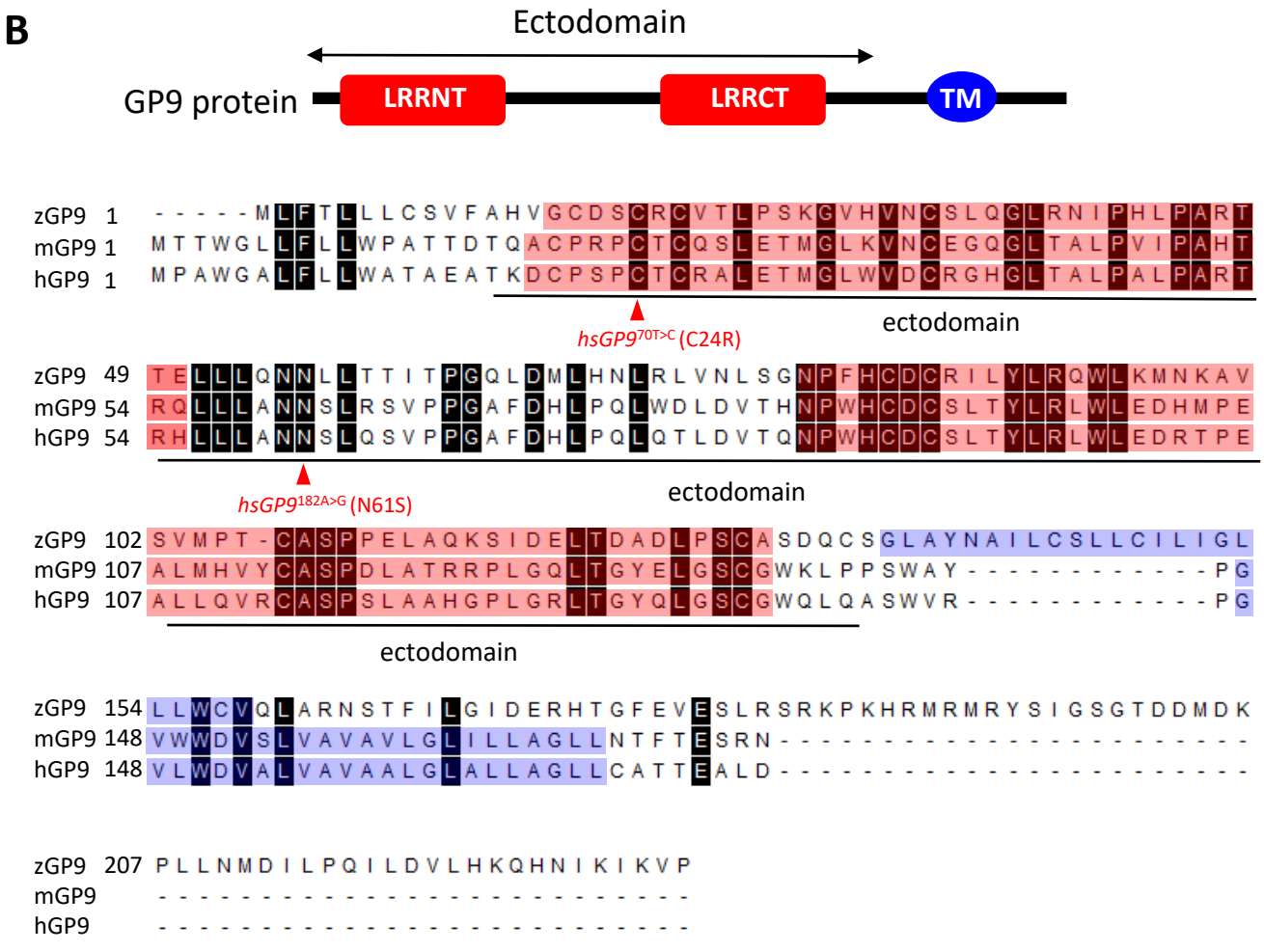
B
Ectodomain
GP9 protein
LRRNT
LRRCT
TM
zGP9 1 - - - - - M L F T L L L C S V F A H V G C D S C R C V T L P S K G V H V N C S L Q G L R N I P H L P A R T
mGP9 1 M T T W G L L F L L W P A T T D T Q A C P R P C T C Q S L E T M G L K V N C E G Q G L T A L P V I P A H T
hGP9 1 M P A W G A L F L L W A T A E A T K D C P S P C T C R A L E T M G L W V D C R G H G L T A L P A L P A R T
ectodomain
hsGP9 70T>C (C24R)
zGP9 49 T E L L L Q N N L L T T I T P G Q L D M L H N L R L V N L S G N P F H C D C R I L Y L R Q W L K M N K A V
mGP9 54 R Q L L L A N N S L R S V P P G A F D H L P Q L W D L D V T H N P W H C D C S L T Y L R L W L E D H M P E
hGP9 54 R H L L L A N N S L Q S V P P G A F D H L P Q L Q T L D V T Q N P W H C D C S L T Y L R L W L E D R T P E
ectodomain
hsGP9 182A>G (N61S)
zGP9 102 S V M P T - C A S P P E L A Q K S I D E L T D A D L P S C A S D Q C S G L A Y N A I L C S L L C I L I G L
mGP9 107 A L M H V Y C A S P D L A T R R P L G Q L T G Y E L G S C G W K L P P S W A Y - - - - - - - - - - - P G
hGP9 107 A L L Q V R C A S P S L A A H G P L G R L T G Y Q L G S C G W Q L Q A S W V R - - - - - - - - - - - P G
ectodomain
zGP9 154 L L W C V Q L A R N S T F I L G I D E R H T G F E V E S L R S R K P K H R M R M R Y S I G S G T D D M D K
mGP9 148 V W W D V S L V A V A V L G L I L L A G L L N T F T E S R N -
hGP9 148 V L W D V A L V A V A A L G L A L L A G L L C A T T E A L D -
zGP9 207 P L L N M D I L P Q I L D V L H K Q H N I K I K V P
mGP9 -
hGP9 -